ORIGINAL ARTICLE

Power law in COVID-19 cases in China

Behzod B. Ahundjanov[1] | **Sherzod B. Akhundjanov[2]** | **Botir B. Okhunjanov[3]**

[1]Department of Economics, University of Illionois, Chicago, Illinois, USA

[2]Department of Applied Economics, Utah State University, Logan, Utah, USA

[3]School of Economic Sciences and Department of Mathematics and Statistics, Washington State University, Pullman, Washington, USA

Correspondence
Sherzod B. Akhundjanov, Department of Applied Economics, Utah State University, 4835 Old Main Hill, Logan, UT 84322-4835, USA.
Email: sherzod.akhundjanov@usu.edu

Abstract

The novel coronavirus (COVID-19) was first identified in China in December 2019. Within a short period of time, the infectious disease has spread far and wide. This study focuses on the distribution of COVID-19 confirmed cases in China—the original epicentre of the outbreak. We show that the upper tail of COVID-19 cases in Chinese cities is well described by a power law distribution, with exponent around one in the early phases of the outbreak (when the number of cases was growing rapidly) and less than one thereafter. This finding is significant because it implies that (i) COVID-19 cases in China is heavy tailed and disperse; (ii) a few cities account for a disproportionate share of COVID-19 cases; and (iii) the distribution generally has no finite mean or variance. We find that a proportionate random growth model predicated by Gibrat's law offers a plausible explanation for the emergence of a power law in the distribution of COVID-19 cases in Chinese cities in the early phases of the outbreak.

KEYWORDS

coronavirus, COVID-19, Gibrat's law, heavy tailedness, Pareto distribution, power law, proportionate random growth

1 | INTRODUCTION

The coronavirus disease 2019 (COVID-19) was first discovered in Wuhan region of China in December 2019 (Zhu et al., 2020). The contagious disease quickly spread within China, despite

unprecedented and aggressive containment measures, and crossed the borders reaching every corner of the world within a short period of time, with the World Health Organization (WHO) declaring COVID-19 outbreak a global pandemic on 11 March 2020 (Cucinotta & Vanelli, 2020). This study focuses on the distribution of COVID-19 confirmed cases in China—the original epicentre of the outbreak—in the first wave of the epidemic. The presence of Chinese cities with very large number of COVID-19 cases, the very wide dispersion in COVID-19 cases across China, and the effect of the pandemic on the economy and welfare make it crucial for researchers and policymakers alike to better understand COVID-19 distribution for effective planning and policy design as well as more efficient use of government resources.

In this article, we demonstrate that the right tail of the distribution of COVID-19 confirmed cases in Chinese cities is well-characterized by a power law (Pareto) distribution, meaning that the probability that a number of COVID-19 cases is more than x is roughly proportional to $x^{-\gamma}$, that is, $\text{Prob}(X > x) \sim x^{-\gamma}$, where γ is the power law (Pareto) exponent. While the estimated power law exponent is $\gamma \simeq 1$ in the early phases of the outbreak, when the number of cases was rising precipitously, it is $\gamma < 1$ thereafter, which indicates the fitted power law distribution in general has no finite moments, including mean and variance. The power law fit is robust to a range of estimation methods and goodness-of-fit tests, and the distribution outperforms several alternative distributions in fitting the data. Power law distributions are characterized by heavy tails, which make the likelihood of extreme (upper tail) events more typical. In case of COVID-19, this implies an extremely large number of cases becomes more likely, which is actually true for China, where a few cities had extremely large number of cases (Han et al., 2020).

Power laws are extraordinarily ubiquitous in the social and natural sciences, having been confirmed for the distributions of income and wealth (Benhabib et al., 2011; Champernowne, 1953; Klass et al., 2006; Pareto, 1896; Singh & Maddala, 1976; Toda, 2012; Wold & Whittle, 1957), consumption (Toda, 2017; Toda & Walsh, 2015), firm size (Axtell, 2001; Luttmer, 2007; Stanley et al., 1995), farmland size (Akhundjanov & Chamberlain, 2019), city size (Berliant & Watanabe, 2015; Devadoss et al., 2016; Gabaix, 1999; Ioannides & Overman, 2003; Krugman, 1996), natural gas and oil production (Balthrop, 2016), carbon dioxide (CO_2) emissions (Akhundjanov et al., 2017), forest fires (Malamud et al., 1998), earthquakes (Bak & Tang, 1989), frequency of words (Irmay, 1997; Zipf, 1949) and even university research activities (Plerou et al., 1999). For a detailed review of power laws, see Reed (2001), Newman (2005), Sornette (2006) and Gabaix (2009, 2016). The omnipresence of power laws is partly explained by the fact that they are preserved over an extensive array of mathematical transformations (Gabaix, 2009). In fact, any multiplicative transformation of this distribution will, in theory, be power law distributed as well. This explains why a power law distribution is also referred to as a scale-free distribution. Our paper contributes to this body of work by presenting evidence for the existence of power law in an epidemiological context.

An interesting aspect of power law distribution is that it is the macro-level steady-state phenomenon that, in theory, can arise from a micro-level proportionate random growth process, known as Gibrat's law (Gibrat, 1931). According to Gibrat's law of proportionate growth, each unit's (e.g. city's) growth rate is drawn randomly and independently of its size, meaning units (whether large or small) on average grow at similar rates. For an in-depth review of Gibrat's law, see Sutton (1997). This empirical regularity, similar to power laws, has been documented extensively in the social and natural sciences. In particular, Gibrat's law has been shown to explain the growth process of consumption (Battistin et al., 2009), firms (Luttmer, 2007), farmland (Akhundjanov & Drugova, 2021), cities (Eeckhout, 2004; Ioannides & Overman, 2003),

countries (González-Val & Sanso-Navarro, 2010; Rose, 2006), carbon dioxide (CO_2) emissions (Ahundjanov & Akhundjanov, 2019) and bird population (Keitt & Stanley, 1998), among others. In this study, we formally test for proportionate random growth at micro-level by analysing growth rates of COVID-19 cases in Chinese cities. We find that a proportionate random growth model is a plausible power law generating mechanism for COVID-19 cases in China in the early phases of the outbreak, when the number of cases was growing. In the later phases of the outbreak, as the number of cumulative cases starts to stabilize, a proportionate random growth model becomes less plausible. This is expected as, after all, Gibrat's law of proportionate growth is a model of growth. As with any theory, we remain cognizant of Gabaix's (2009) remark that, 'the main question of empirical work should be how well a theory fits, rather than whether it fits perfectly'.

There are a couple of noteworthy implications of the findings presented in this article. First, and foremost, the analysis uncovers potential heavy tailedness and tail risk property in COVID-19 cases in Chinese cities, which has a direct implication for empirical research. Specifically, it shows that thin-tailed distributions (e.g. the normal) are *not* appropriate for COVID-19 cases in Chinese cities as such distributions dismiss extremely large number of cases as an improbable observation. Our analysis reveals that even some, more common heavy-tailed distributions (e.g. the lognormal and exponential) are not plausible in this context. This is important because distributions like normal or lognormal are often 'go-to' distributions in empirical work, and the trend of adopting these distributions with little or no a priori justification or on the basis of convenience has been observed in the rapidly expanding COVID-19 literature. On the other hand, a power law distribution is able to capture the heavy upper tail of the data more closely, outperforming a number of alternative distributions. For sound analysis of the effects of COVID-19 pandemic, using statistically justified and robust methods that account for possible heavy tailedness and tail risk properties is integral (Distaso et al., 2020).

Second, given that the estimated Pareto exponent is generally less than one ($\gamma < 1$) towards the end of the first wave of the pandemic, the distribution of COVID-19 cases in Chinese cities is heavy tailed and so disperse that observations near the mean account for little of the cumulative distribution of COVID-19 cases. This implies talking about the typical or average number of COVID-19 cases is inconsequential as it does not represent the majority of cases. In fact, even though it is possible to compute sample mean and variance for the observed data, these moments are generally non-convergent. Therefore, the distribution of COVID-19 cases (as of the end of the first wave of the pandemic) cannot be well characterized by quoting its mean and variance. Instead, quantile analysis or order statistics would be a more appropriate approach to describing the data.

Finally, the heavy upper tail of the distribution is suggestive of concentration of COVID-19 cases in China, with the total cases essentially being determined by a few cities that bore the brunt of the outbreak, which is true in case of China (Han et al., 2020). This has implications for more effective epidemiological planning and policy design as by directing resources to disease epicentres (i.e. cities located in the upper tail), the spread of the outbreak can potentially be contained or, at least, slowed. Moreover, by understanding characteristics of these upper-tail cities that make them especially prone to the infection, more effective preventative measures can be designed and implemented to combat possible subsequent waves of the pandemic.

The literature in this area is thin, but gradually forming. In the concurrent work, Beare and Toda (2020), studying the distribution of COVID-19 confirmed cases for US counties, find that the upper tail of this distribution follows a power law, with Pareto exponent close to 1.

Similarly, Blasius (2020), examining the distribution of COVID-19 confirmed cases and deaths for US counties, concludes that both distributions exhibit a power law behaviour. Our paper contributes to this nascent line of literature by exploring the distribution of COVID-19 confirmed cases in China—the origin of the outbreak. A distinctive feature of our study is that COVID-19 cases in China affords us to capture the entire life cycle of the pandemic (at least in its first wave): outbreak detection, spread, peak and decline to zero new daily cases. In contrast, the analyses presented in Beare and Toda (2020) and Blasius (2020) are based on datasets that were largely evolving at the time, as both the United States and a whole host of other countries were battling to contain the spread of the virus when these articles were initially written. Thus, the results of the above studies are likely subject to change with newer data.

The remainder of the paper is structured as follows. Section 2 introduces the data for the analysis. Section 3 presents the methods and findings for power law analysis. Section 4 reviews a mechanism that can generate power law distribution, and discusses its plausibility in the case examined in this study. Section 5 provides some concluding remarks.

2 | DATA

Daily data on the cumulative number of COVID-19 confirmed cases for Chinese cities come from Harvard Dataverse (China Data Lab, 2020). The dataset includes 339 cities in China and tracks the COVID-19 cases starting from 15 January 2020. Our main analysis focuses on COVID-19 cases as of 23 May 2020, the latest data on cumulative cases at the time of writing this article. By 23 May 2020, the number of cumulative cases in China had stabilized, with zero new daily cases, which suggests the containment of the first wave of the outbreak in the country. Our analysis thus allows us to understand the distribution of COVID-19 cases in its first complete life cycle.

Figure 1 shows the location of Chinese cities with confirmed COVID-19 cases as of 23 May on the map of China. As illustrated in Figure 2, most Chinese cities in the sample had reported a positive number of cases by 8 February 2020. Figure 3 shows the evolution of empirical distribution of COVID-19 cases in Chinese cities over select dates. It is apparent that the distribution has been right skewed, with heavier right tail. Also, the distribution has been gradually sliding rightward over time, which reflects growing number of COVID-19 cases across Chinese cities.

In Figure 4, we plot the ratio of COVID-19 cases to population size in Chinese cities between 15 January 2020 and 23 May 2020. We use the 2020 population data for Chinese cities collected from United Nations (2018). It is evident that COVID-19 cases represented a minute fraction of total population of each city throughout the study period, with majority of cities having less than 0.00025 fraction of their population infected by the virus. Even Wuhan, a city pummeled by the outbreak, had only 0.006 fraction of its population with confirmed COVID-19 infection by the end of the first wave of the pandemic. This shows that the population of cities in the beginning, and throughout the first wave, of the epidemic does not limit its spread, meaning the population of cities can effectively be treated as 'infinite' relative to COVID-19 cases.

A power law analysis is data intensive, with Clauset et al. (2009) recommending a minimum of 50 observations for reliable analysis. This condition is well-satisfied here, including for the upper tail of our sample, as discussed further below.
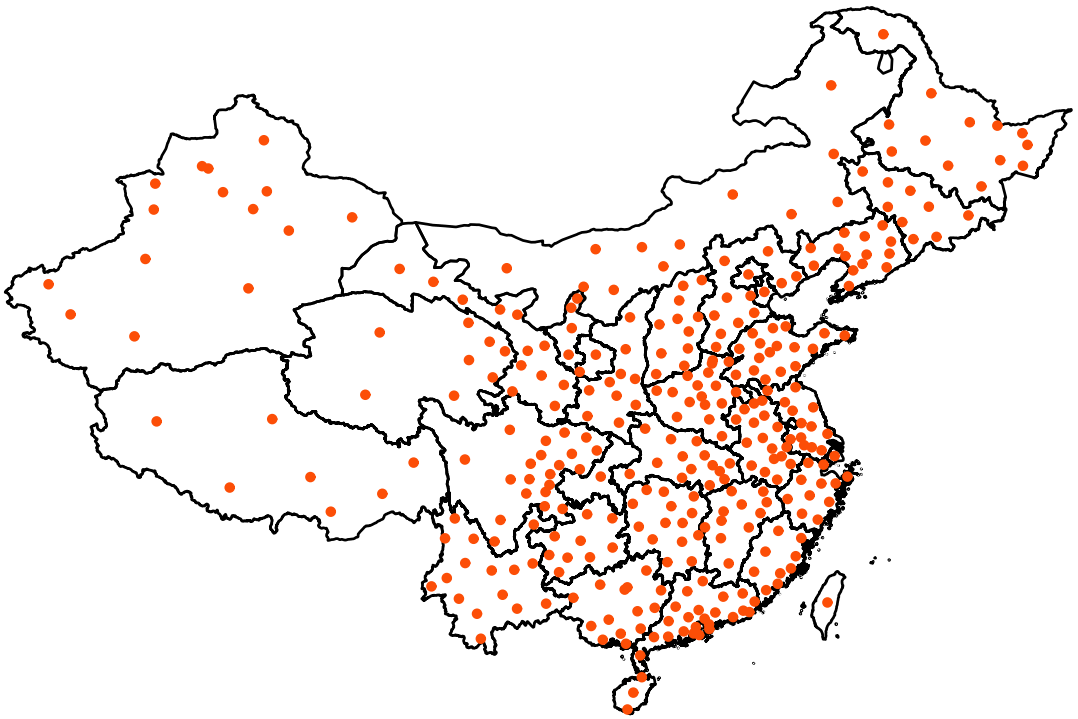
FIGURE 1 Chinese cities with confirmed COVID-19 cases as of May 23, 2020
Data source: Harvard Dataverse (China Data Lab, 2020) [Colour figure can be viewed at wileyonlinelibrary.com]

3 | POWER LAW ANALYSIS

In this section, we examine the distribution of the cumulative number of COVID-19 confirmed cases for Chinese cities. We first present the methodology for power law analysis, followed by estimation results and diagnostics.

3.1 | Power law parameter estimation

Suppose X is a random variable whose data generating process is a continuous power law (Pareto) distribution. The corresponding probability distribution function (PDF) is specified as

$$f(x) = \frac{\alpha - 1}{x_{\min}} \left(\frac{x}{x_{\min}} \right)^{-\alpha}, \tag{1}$$

where x is an outcome of X for $x \in \mathbb{R}_+$, where $\mathbb{R}_+ = \{x \in \mathbb{R} | x > 0\}$, $x_{\min}$ is the threshold beyond which (i.e. $x \geq x_{\min}$) power law behaviour sets in, and α is the power law (Pareto) exponent, which is a parameter of interest. The mth non-central moment for the power law distribution is given by

$$\langle x^m \rangle = \int_{x_{\min}}^{\infty} x^m f(x) dx = \left(\frac{\alpha - 1}{\alpha - 1 - m} \right) x_{\min}^m, \quad \forall \alpha > m + 1. \tag{2}$$
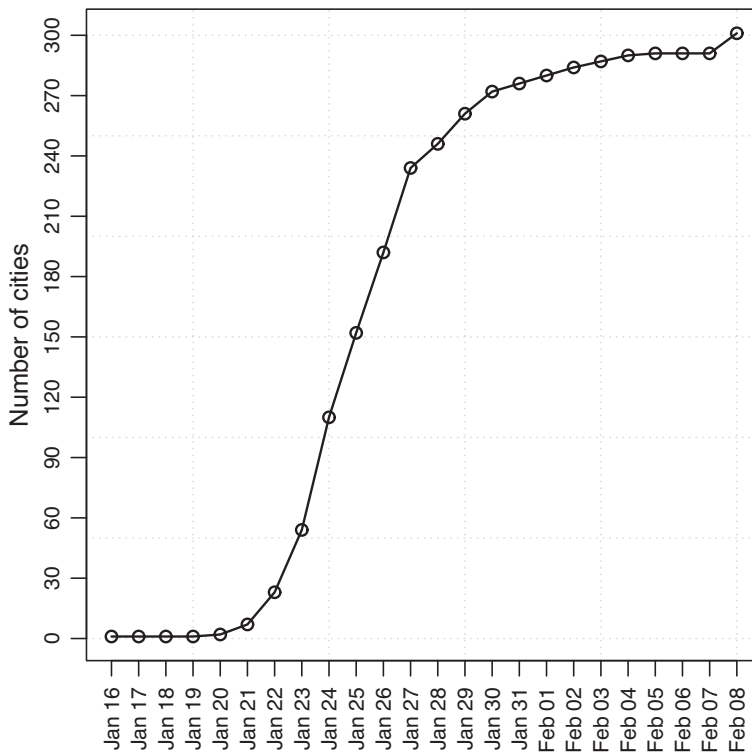
FIGURE 2 The number of Chinese cities with confirmed COVID-19 cases over time
Data source: Harvard Dataverse (China Data Lab, 2020)

Hence only the first $\lfloor\alpha-1\rfloor$ moments exist for $m < \alpha - 1$. Although higher order moments can be calculated for any finite sample, these estimates do not asymptotically converge to any particular value. Given the sample $x_1, \ldots, x_n$, the joint log-likelihood function can be written as

$$\ln \mathcal{L}(\alpha; x_1, \ldots, x_n) = \sum_{i=1}^{n} \left[\ln(\alpha - 1) - \ln x_{\min} - \alpha \ln \frac{x_i}{x_{\min}} \right]$$

$$= n \ln(\alpha - 1) - n \ln x_{\min} - \alpha \sum_{i=1}^{n} \ln \frac{x_i}{x_{\min}}. \tag{3}$$

First-order condition yields the maximum likelihood estimate (MLE) of

$$\alpha^{MLE} = 1 + n \left(\sum_{i=1}^{n} \ln \frac{x_i}{x_{\min}} \right)^{-1} \tag{4}$$

with the standard error (SE) of the estimate given by

$$SE(\alpha^{MLE}) = \sqrt{n} \left(\sum_{i=1}^{n} \ln \frac{x_i}{x_{\min}} \right)^{-1} = \frac{\alpha^{MLE} - 1}{\sqrt{n}}. \tag{5}$$
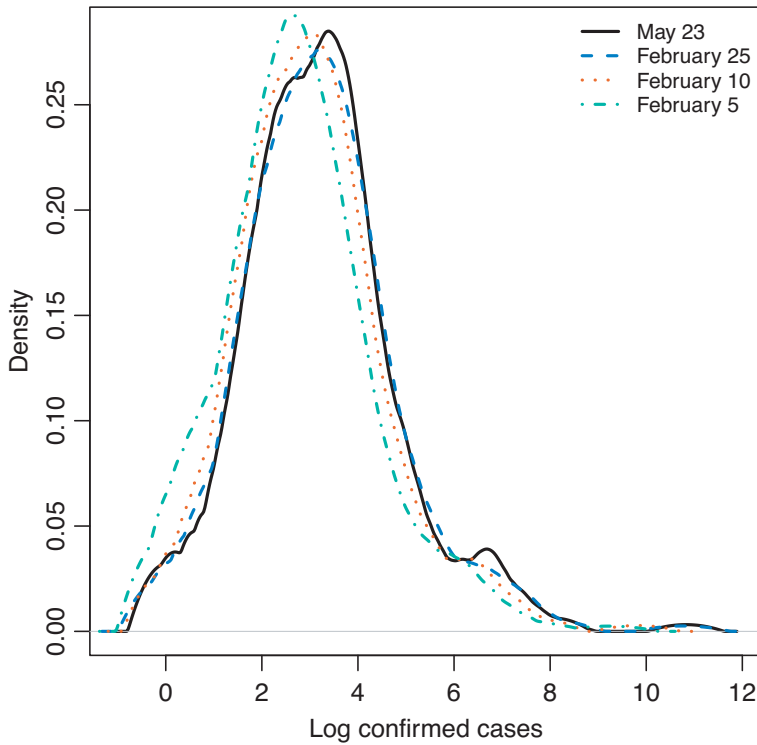
F I G U R E 3 The empirical distribution of cumulative number of COVID-19 confirmed cases for Chinese cities. The empirical distribution is obtained using kernel density with Epanechnikov kernel and the smoothing bandwidth based on unbiased cross-validation method [Colour figure can be viewed at wileyonlinelibrary.com]

It is standard to report the counter-cumulative parameter $\gamma = \alpha^{MLE} - 1$, known as the Hill estimator (Hill, 1975), instead of Equation (4). The Hill estimator, which is obtained from Equation (4) after a small-sample adjustment, takes the following form

$$\gamma^{Hill} = \frac{n-2}{\sum_{i=1}^{n-1}(\ln x_i - \ln x_{\min})} \tag{6}$$

with the standard error of the estimate given by

$$SE(\gamma^{Hill}) = \frac{\gamma^{Hill}}{\sqrt{n-3}}. \tag{7}$$

The power law fit to data is typically illustrated by plotting the counter-cumulative distribution function (counter-CDF)—also known as the survival function—on doubly logarithmic axes. The counter-CDF of a power law is specified as

$$\text{Prob}(X > x) = \left(\frac{x}{x_{\min}}\right)^{-\alpha+1} = \frac{k}{x^\gamma}, \tag{8}$$
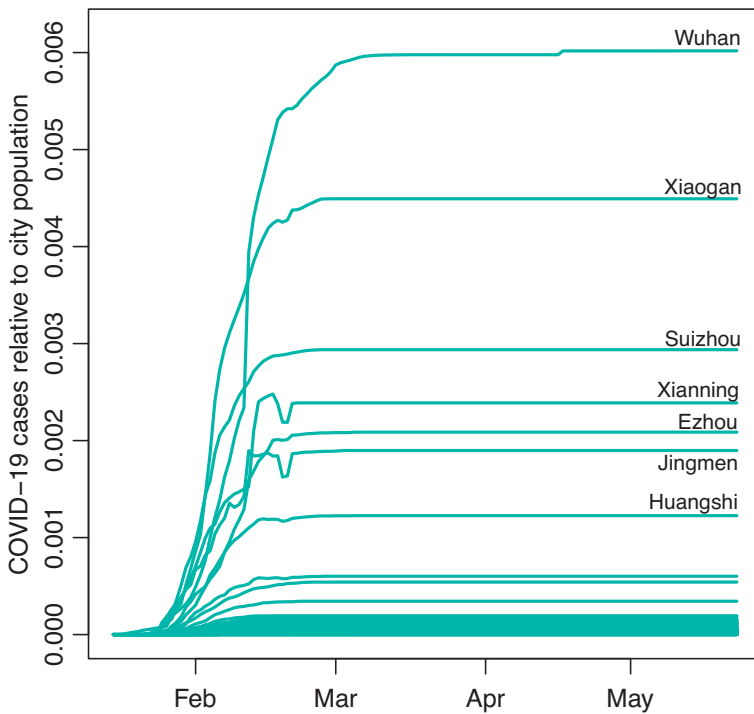
FIGURE 4　The ratio of COVID-19 cases to city population in China between 15 January 2020 and 23 May 2020 [Colour figure can be viewed at wileyonlinelibrary.com]

where $k = x_{\min}^{\alpha-1}$ is a constant. Taking the log of both sides of (8) yields a well-known linear relationship between log counter-cumulative probability (i.e. $\ln \text{Prob}(X > x)$) and log data (i.e. $\ln x$), with the counter-cumulative parameter $-\gamma$ being the slope of the line.

An alternative approach to estimating the counter-cumulative parameter γ is through a regression-based technique. Specifically, estimate the following regression equation with ordinary least squares (OLS)

$$\ln(rank_i) = \phi - \gamma^{OLS} \ln x_i + \varepsilon_i, \tag{9}$$

where $rank_i$ is observation i's rank in the distribution, ϕ is the intercept term, γ^{OLS} is the parameter of interest, and ε_i is the idiosyncratic disturbance term. Equation (9) also shows that a power law distributed process appears approximately linear on a log–log plot of $rank_i$ against x_i, with slope of $-\gamma^{OLS}$. The asymptotic standard error for γ^{OLS} is given by (Gabaix & Ibragimov, 2011)

$$SE(\gamma^{OLS}) = \frac{\gamma^{OLS}}{\sqrt{n/2}}. \tag{10}$$

An important consideration in power law analysis is the specification of the threshold parameter $x_{\min}$, beyond which power law behaviour takes hold. There are several approaches proposed in the literature in this regard. For instance, one strand of literature suggests to select $x_{\min}$ at either the 95% quantile of the data or the point where empirical PDF or CDF roughly straightens out on a log–log plot (Gabaix, 2009). Another strand of the literature simply uses the largest $\sqrt{n}$ or $n/10$ observations in the analysis (Farmer et al., 2004). Clearly, these approaches are rather arbitrary and thus suffer from a certain degree of uncertainty about whether they can capture the

true starting point of power law behaviour. If the arbitrarily selected x_{min} is smaller than the true value of x_{min}, the estimate of power law exponent will be biased as it attempts to fit non-power law data to a power law model. Conversely, if x_{min} exceeds the point where the true power law behaviour begins, it results in discarding valuable data and causes the standard error to increase. Importantly, Perline (2005), investigating the empirical consequences of this concern, shows that sufficiently truncated Gumbel-type distributions (e.g. the lognormal) can also produce a linear pattern on a log–log plot, hence imitating the power law distribution.

We adopt a more systematic, data-driven procedure to select x_{min} (Clauset et al., 2009). The main advantage of this method is that it allows the analyst to identify the power law portion of the data (if any) in a more objective and principled manner, balancing the trade-off between setting x_{min} too small or too high relative to the true value of x_{min}. This approach essentially treats each observation in the sample as a potential candidate for x_{min} and selects the best candidate based on the minimization of the Kolmogorov–Smirnov (KS) goodness-of-fit statistic, which is given by

$$KS = \max_{x \geq x_{min}} |E(x) - \hat{F}(x)|. \tag{11}$$

In Equation (11), $E(x)$ is the empirical CDF and $\hat{F}(x)$ is the estimated power law CDF. The optimal x_{min} minimizes the distance between the empirical CDF and the estimated power law CDF. The computational algorithm takes the following form:

Step 1: Set $x_{min} = x_1$;
Step 2: Perform power law parameter estimation using $x \geq x_{min}$;
Step 3: Compute the KS statistic in Equation (11);
Step 4: Repeat steps 1–3 for all x_i for $i = 1, \ldots, n$;
Step 5: Select x_{min} with the lowest KS statistic.

3.2 | The goodness-of-fit tests

Significant parameter estimates alone do not provide sufficient evidence in favour of power law fit to data. Power law analysis is accompanied by a series of diagnostic tests. To guard against potential misspecification issues, one needs to conduct a goodness-of-fit test and compare the power law fit to data with those of alternative distributions.

Gabaix and Ibragimov (2011) proposed 'rank − 1/2' test to verify the goodness-of-fit of power law distribution. Let x^* be defined as

$$x^* = \frac{\text{Cov}[(\ln x_i)^2, \ln x_i]}{2 \, \text{Var}(\ln x_i)}. \tag{12}$$

Then, regress bias-adjusted log rank against the log data and a quadratic deviation term, as in

$$\ln \left(rank_i - \frac{1}{2} \right) = \phi + \zeta \, \ln x_i + q(\ln x_i - x^*)^2 + \epsilon_i. \tag{13}$$

The goodness-of-fit statistic is specified as q/ζ^2. The null hypothesis of power law distributedness is rejected if $q/\zeta^2 > 1.95(2n)^{-1/2}$, where the latter term is the goodness-of-fit threshold.

Furthermore, Clauset et al. (2009) suggest comparing power law fit with those of other competing (heavy-tailed) distributions, such as the lognormal and exponential. Accordingly, we fit these alternative distributions to the data by MLE and provide visual comparisons of the distributions' fits on a doubly logarithmic plot as detailed above. In addition to conventional model fit measures, such as the Akaike information criterion (AIC) and Bayesian information criterion (BIC), we also implement the likelihood ratio test of Clauset et al. (2009) for a formal comparison. The likelihood ratio statistic is specified as

$$\mathcal{R} = \sum_{i=1}^{n} \left[\ln \hat{f}_1(x_i) - \ln \hat{f}_2(x_i) \right], \tag{14}$$

where $\hat{f}_1(x_i)$ and $\hat{f}_2(x_i)$ are the probabilities predicted by power law and an alternative distribution respectively. If the likelihood ratio statistic is positive, it indicates the power law distribution fits the data more closely. If it is negative, then an alternative distribution yields a better fit. For other properties of the likelihood ratio statistic, including its advantage over other goodness-of-fit measures and the derivation of its p-value, see Clauset et al. (2009).

3.3 | Application

The methods discussed in Sections 3.1 and 3.2 are applied to the cumulative number of COVID-19 confirmed cases in Chinese cities (x) as of 23 May 2020. We omit cities with zero COVID-19 cases as of 23 May 2020, from the dataset. The main results from power law analyses appear in Tables 1 and 2 and Figure 5. The KS estimate of $x_{\min}$ is 24, as reported in Table 1. Consequently, 151 observations out of 339, which satisfy $x \geq 24$, are used in power law analysis. As noted earlier, the requirement placed on sample size for credible power law analysis is a minimum of 50 observations (Clauset et al., 2009). This condition is well-satisfied here. The Hill and OLS estimates of the counter-cumulative parameter γ are around 0.80 and statistically different from zero. Given $m < 0.80$, the moments of the fitted power law distribution (including mean and variance) are generally non-convergent. The goodness-of-fit test of Gabaix and Ibragimov (2011) suggests we fail to reject the null hypothesis of power law distributedness of COVID-19 cases in China.

Figure 5 depicts the power law and competing heavy-tailed distributions' fits to the data. It is clear that the power law distribution generally fits the data better than the rivalling distributions, particularly in the lower to mid quantiles of the upper tail, where the observed data form a distinct linear pattern. The power law slightly overestimates the frequency of the largest cases in the extreme upper tail (after log confirmed cases of about 7.8), where the fitted distribution decays relatively slowly. The fits of competing distributions—the lognormal and exponential—noticeably deviate from the empirical data throughout the domain. Formal goodness-of-fit measures in Table 2 provide further support in this regard. As is evident from AIC and BIC, as well as large positive likelihood ratio statistics, the power law distribution markedly outperforms both the lognormal and exponential distribution in fitting COVID-19 cases in China, which is in line with our observations from Figure 5. Therefore, we reject both the lognormal (and, by extension, the normal) and exponential as an adequate specification for COVID-19 cases in Chinese cities.

In order to verify the sensitivity of our findings to the (data-driven) choice of $x_{\min}$, we next perform power law estimation and diagnostics with alternative candidates for $x_{\min}$. Figure 6 presents

TABLE 1 Power law parameter estimates and goodness-of-fit test

	Estimate	Standard error
γ^{Hill}	0.808	(0.066)
γ^{OLS}	0.762	(0.087)
$x_{\min}$	24	
Observations ($x > x_{\min}$)	151	
Observations (total)	339	
The Gabaix and Ibragimov goodness-of-fit test		
Goodness-of-fit test statistic	0.013	
Goodness-of-fit threshold	0.112	

Notes: Estimation is based on upper-tail observations $x > x_{\min}$ as of 23 May 2020, where $x_{\min}$ is determined based on the minimization of the KS statistic. For the Gabaix and Ibragimov (2011) test, the null hypothesis that COVID-19 confirmed cases is distributed according to a power law is rejected if a goodness-of-fit statistic is greater than a corresponding threshold value. Clauset et al. (2009) recommend to have at least 50 observations for accurate power law analysis, a condition satisfied here.

TABLE 2 Model fit measures of competing distributions

	Log-likelihood	AIC	BIC	Likelihood ratio statistic	*p*-value
Power law	−845.545	1,693.089	1,696.106		
Exponential	−1,097.721	2,197.441	2,200.459		
Lognormal	−1,174.851	2,353.702	2,359.736		
Power law versus exponential				252.176	0.002
Power law versus lognormal				329.306	0.000

Notes: Estimation is based on upper-tail observations $x > x_{\min}$ as of 23 May 2020, where $x_{\min}$ is determined based on the minimization of the KS statistic. A positive value of the likelihood ratio statistic indicates that the power law is the better fitting distribution. A negative value indicates the alternative distribution fits the data more closely. *p*-values are calculated using the methods detailed in Clauset et al. (2009). The null hypothesis is that there are no significant differences in likelihoods of the distributions tested.

our results, where, as reflected by the horizontal axes, we treat each observation in the sample as a potential choice for $x_{\min}$. In panels (a) and (b), we plot the Hill and OLS estimates, respectively, of power law parameter γ as a function of $x_{\min}$. This amounts to what is commonly known as a Hill plot, which is a visual approach to choosing $x_{\min}$ (Clauset et al., 2009). Given the estimates of γ appear roughly stable beyond the data-driven choice of $x_{\min}$ (i.e. the vertical dashed line), this suggests that the data-driven choice of $x_{\min}$ is also plausible under the visual selection technique of $x_{\min}$. Furthermore, the goodness-of-fit tests in panels (c) and (d) establish that for *any* choice of $x_{\min}$: (i) we consistently fail to reject the null hypothesis of Gabaix and Ibragimov (2011) goodness-of-fit test, and (ii) the power law fit emerges superior according to BIC (and AIC, which is omitted in the interest of space). This illustrates the robustness of our observation that the distribution of COVID-19 cases in China is consistent with the characterization of power laws.

Lastly, we conduct a power law analysis through time to show a development, and possible trend, in power law exponent γ. This exercise also helps us test the robustness of our main finding to temporal variations and idiosyncrasies in the sample of COVID-19 cases in China. We fit the model to each day between 15 January 2020 and 23 May 2020, with $x_{\min}$ identified for each date using the method detailed in Section 3.1. According to panels (a) and (b) of Figure 7, the estimated
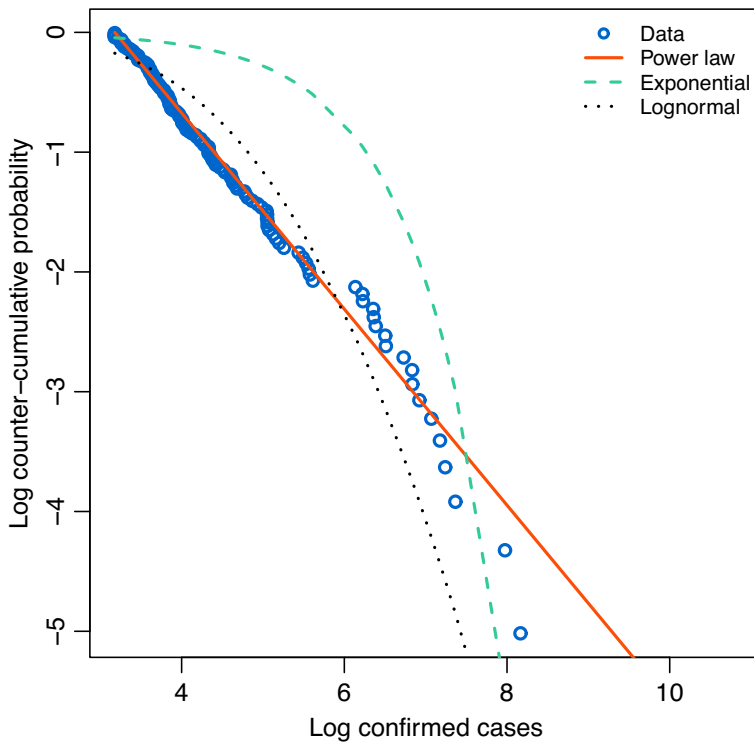
FIGURE 5   Plot of empirical and fitted log counter-cumulative probability and log COVID-19 confirmed cases. Estimation is based on upper-tail observations $x > x_{min}$ as of 23 May 2020, where x_{min} is determined based on the minimization of the KS statistic [Colour figure can be viewed at wileyonlinelibrary.com]

value of power law parameter γ grows rapidly during the early days of the pandemic, when the virus was spreading most intensely, with the estimates of γ hovering around unity between late January and early February. By mid-February, the COVID-19 situation in China largely stabilized, which explains the trend forming around $\gamma \simeq 0.8$ in the period thereafter. Of particular interest for our subsequent analysis is the observation that $\gamma \simeq 1$ in the early phases of the outbreak. This indicates the existence of a *finite* mean for the distribution of COVID-19 cases in China during that time frame. Moreover, the diagnostic tests in panels (c) and (d) of Figure 7 indicate that the power law fit to COVID-19 cases in Chinese cities is remarkably robust over the first wave of the pandemic: (i) we consistently fail to reject the null hypothesis of Gabaix and Ibragimov (2011) goodness-of-fit test, and (ii) the power law fit remains superior according to BIC (and AIC, which is omitted in the interest of space). This shows that our main results reported in Tables 1 and 2 and Figure 5 are not driven by the nature of a sample used in that analysis, but rather power law is a genuine phenomenon in this case. Granted that the number of confirmed cases is affected by the underlying infective process as well as detection process, the power law analysis through time also establishes the robustness of our main finding to any potential changes in the detection process of COVID-19 cases over the course of the first wave of the pandemic.

It is worth mentioning that the distribution in Equation (1) is a representative from the class of regularly varying distributions (i.e. general power law). The power law estimation framework presented in this study is consistent under the assumption that a given data comes from a pure power law, which forms a small subset of general power laws. On the other hand, the estimation framework reviewed in Voitalov et al. (2019) is shown to be consistent under the more general
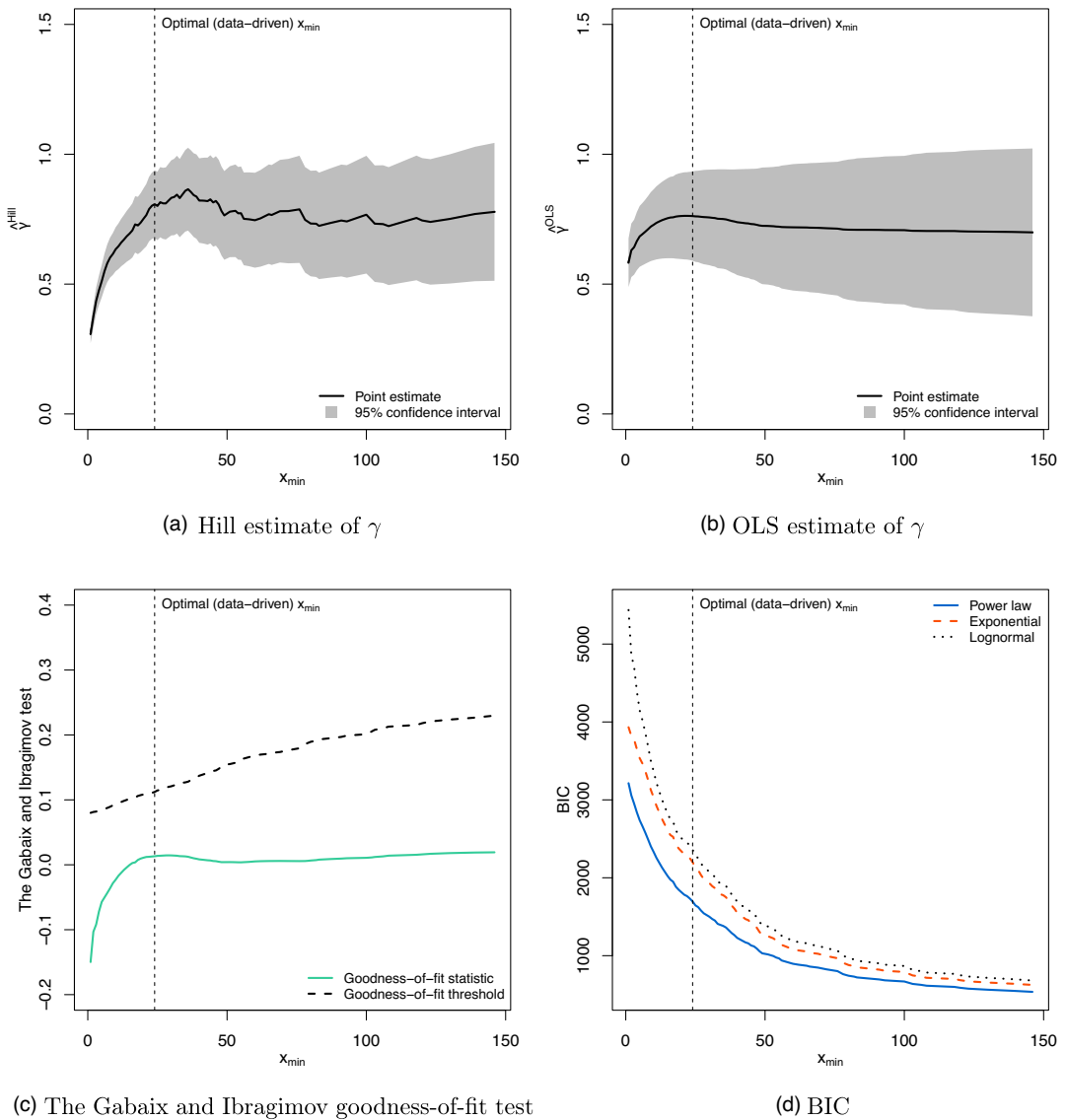
(a) Hill estimate of γ

(b) OLS estimate of γ

(c) The Gabaix and Ibragimov goodness-of-fit test

(d) BIC

FIGURE 6 Sensitivity analysis with the choice of x_{min}. Estimation for each given choice of x_{min} is based on upper-tail observations $x > x_{min}$ as of 23 May 2020. The vertical (dashed) line indicates the position of optimal (data-driven) choice x_{min}. For the Gabaix and Ibragimov (2011) test, the null hypothesis that COVID-19 confirmed cases is distributed according to a power law is rejected if a goodness-of-fit statistic is greater than a corresponding threshold value [Colour figure can be viewed at wileyonlinelibrary.com]

assumption that the data comes from any impure power law. Indeed, there are more flexible forms of the Pareto distribution—often with an extra parameter and/or of mixture form—that allow for capturing extreme upper-tail (and lower-tail) probabilities more closely. Such generalized, or, composite, distributions have been shown to improve upon the benchmark power law distribution in fitting empirical data (see, for instance, Giesen et al., 2010; Ioannides & Skouras, 2013; Luckstead & Devadoss, 2017; Nigai, 2017; Patel & Schoenberg, 2011). The main goal of the present study is to determine whether a power law generally approximates the *upper tail* COVID-19 cases in China, which has an implication for understanding tail risk properties of COVID-19, and not
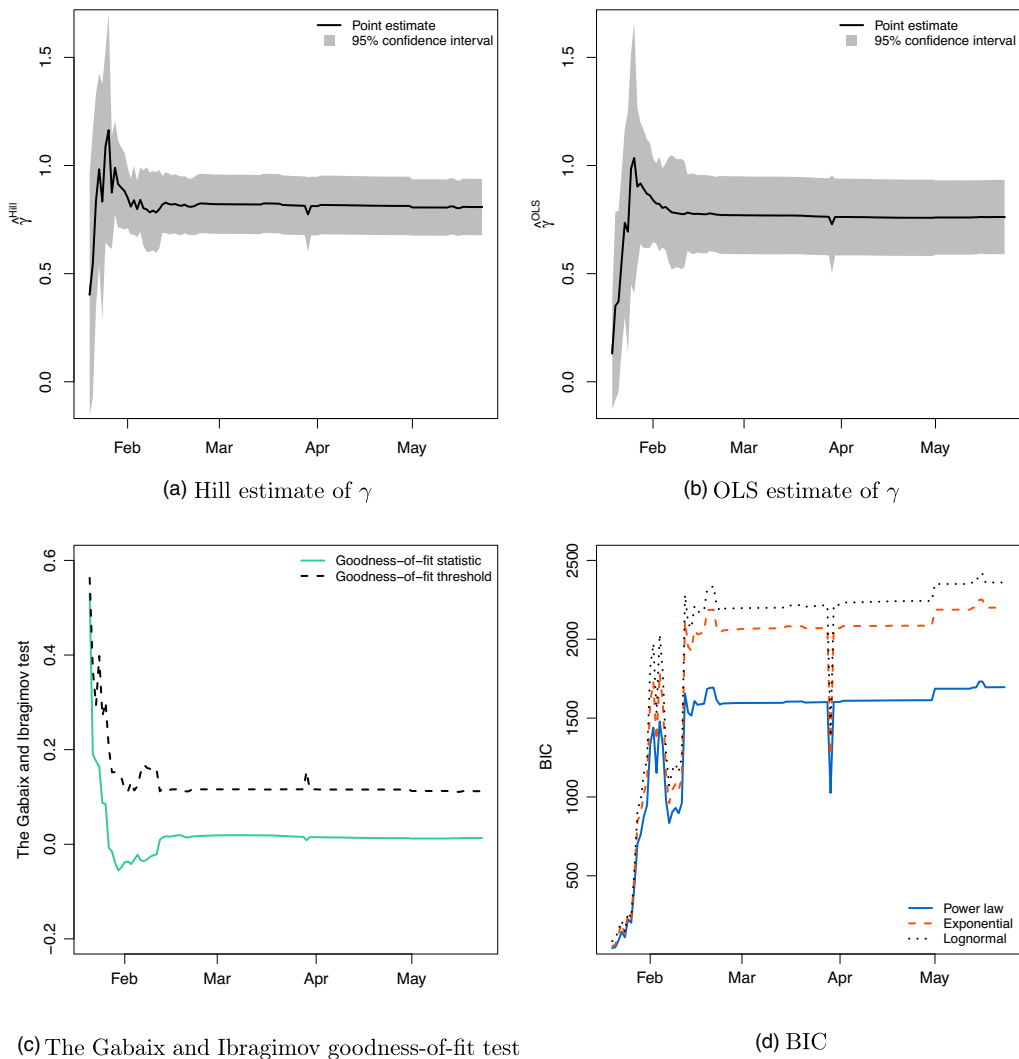
(a) Hill estimate of γ

(b) OLS estimate of γ

(c) The Gabaix and Ibragimov goodness-of-fit test

(d) BIC

FIGURE 7   Power law analysis over the first wave of the pandemic. Estimation is based on upper-tail observations $x > x_{min}$ on each day, where x_{min} for each date is determined based on the minimization of the KS statistic. For the Gabaix and Ibragimov (2011) test, the null hypothesis that COVID-19 confirmed cases is distributed according to a power law is rejected if a goodness-of-fit statistic is greater than a corresponding threshold value [Colour figure can be viewed at wileyonlinelibrary.com]

the investigation of various distributions within the power law family, which is beyond the scope of this research. Our estimation results and diagnostic tests provide empirical evidence that the right tail of COVID-19 cases in Chinese cities is well-characterized by the power law (Pareto) distribution.

4 | EXPLAINING A POWER LAW IN COVID-19 CASES IN CHINA

There are different mechanisms proposed in the literature that can generate power laws. For a thorough review, see Reed (2001), Mitzenmacher (2004), Newman (2005), and Gabaix (2016).

In this section, we explore whether a growth model involving Gibrat's law (Gibrat, 1931) can potentially explain the emergence of the observed power law behaviour in COVID-19 cases in China. We focus on Gibrat's law specifically granted that a random multiplicative growth is the prevalent attribute of models explaining the genesis of power laws (Gabaix, 1999, 2009; Reed, 2001).

4.1 | A link between power law and Gibrat's law

Suppose S_{it} is the size of a stochastic process of interest for unit i at time t. For instance, COVID-19 cases in city i up to day t. According to Gibrat's law, the size of the process (at least in the upper tail) exhibits random multiplicative growth, evolving as

$$S_{it+1} = \mu_{it+1} S_{it} \tag{15}$$

over time, where μ_{it+1} is independently and identically distributed (i.i.d.) random variable with an associated PDF of $f(\mu)$. Hence, random growth factor $\mu_{it+1} = S_{it+1}/S_{it}$ is independent of the current size S_{it}, which is commonly known as Gibrat's law of proportionate growth. Gibrat's law alone is not sufficient to give rise to a power law. In fact, it leads to the lognormal distribution, which was noted by Gibrat (1931) himself early on. Interestingly, many examples used by Gibrat (1931) have recently been shown to actually follow a Pareto-type distribution rather than the lognormal (Akhundjanov & Toda, 2020). Gabaix (1999) showed that power law can arise from Gibrat's law with an auxiliary assumption, a sketch of which we provide below.

Let $G_t(s) = \text{Prob}(S_t > s)$ be the counter-CDF of S_t. Substituting Equation (15) into the counter-CDF, the equation of motion for $G_{t+1}(s)$ boils down to

$$\begin{aligned} G_{t+1}(s) &= \text{Prob}(S_{t+1} > s) \\ &= \text{Prob}\left(S_{it} > \frac{s}{\mu_{t+1}}\right) \\ &= \int_0^\infty G_t\left(\frac{s}{\mu}\right) f(\mu) \, d\mu. \end{aligned} \tag{16}$$

If there is a steady state process $G_t = G$, then

$$G(s) = \int_0^\infty G\left(\frac{s}{\mu}\right) f(\mu) \, d\mu. \tag{17}$$

The mechanism ensuring that power law distribution is the (only) suitable steady state distribution in Equation (17) is if S_t has lower reflecting barrier $S_{\min}$, that is, the minimal size of the process, such that $S_t > S_{\min}$ (Gabaix, 1999, Proposition 1). In this case, $G(s) = \frac{k}{x^\gamma}$, from Equation (8). Thus, Gibrat's law combined with a lower bound on S_t can plausibly yield power law distribution.

The standard theory of proportionate random growth is valid if the mean of the stationary distribution is finite (Gabaix, 1999, 2009). Our analysis in Section 3.3 uncovers a power law in COVID-19 cases (as of 23 May 2020) with no finite mean, which seemingly indicates that the specific power law for COVID-19 cases in China cannot be generated by the standard

model for Gibrat's law of proportionate growth. But, as our temporal power law analysis has demonstrated (see Figure 7), the fitted power law distribution does have a finite mean during the early phases of the outbreak (as $\gamma \simeq 1$), when the number of confirmed cases was rising. This implies a proportionate random growth model can offer a possible explanation for the emergence of a power law in the distribution of COVID-19 cases in the early phases of the outbreak. In the later phases of the outbreak, as the number of cumulative cases starts to stabilize, a proportionate random growth model becomes less and less plausible, as $\mathbb{E}(\mu_{it}) = 1$ in Equation (15). This is anticipated as, after all, Gibrat's law of proportionate growth is a model of growth. Therefore, we formally test for proportionate random growth at micro-level by analysing growth rates of COVID-19 cases in Chinese cities during the early days of the pandemic.

4.2 | Testing for Gibrat's law

For empirical purposes, we consider a continuous time representation of Gibrat's law, given by geometric Brownian motion

$$dS_{it} = gS_{it}dt + \nu S_{it}dB_{it}, \tag{18}$$

where g is the expected growth rate, $\nu > 0$ is the volatility, and B_{it} is a standard Brownian motion that is i.i.d. across cross-sectional units. Applying Itô's lemma to Equation (18) yields

$$d \ln S_{it} = (g - \nu^2/2)dt + \nu dB_{it}, \tag{19}$$

meaning the cross-sectional distribution of S_{it}, with the initial size of S_{i0}, is lognormal

$$\ln(S_{it}/S_{i0}) \sim N[(g - \nu^2/2)t, \nu^2 t]. \tag{20}$$

Equation (19), along with Proposition 1 in Gabaix (1999), suggests that growth rates under Gibrat's law can be described by a random walk process of the form (Eeckhout, 2004; Gabaix, 2009; Sutton, 1997)

$$\ln S_{it} = \ln S_{it-1} + \zeta_{it}. \tag{21}$$

Setting the random growth component $\zeta_{it} = \phi_i + \xi_{it}$, where ϕ_i is the effect of unit-wide factors and ξ_{it} is an i.i.d. random effect, produces a random walk with drift. A standard method to test for Gibrat's law is through estimation of the following cross-sectional regression equation

$$\ln S_{it} = \phi + \rho \ln S_{it-1} + \xi_{it}. \tag{22}$$

In Equation (22), ρ is the parameter of interest, with $\rho \simeq 1$ providing statistical evidence that the growth process of S_t adheres to Gibrat's law.

An alternative approach for testing for proportionate random growth is through estimation of the cross-sectional regression equation of the form

$$\Delta \ln S_{it+1} = \beta_{0t} + \beta_{1t} \ln S_{it} + \beta_{2t}\Delta \ln S_{it} + \beta_3 D_{it} + e_{it}, \tag{23}$$

where Δ is the difference operator, $\Delta \ln S_{it+1}$ is the COVID-19 growth rate in city i between day t and $t + 1$, $\Delta \ln S_{it}$ is the COVID-19 growth rate in city i between day $t - 1$ and t, D_{it} is the number of days between day t and the day of the first COVID-19 case in city i, and e_{it} is an i.i.d. error term. The parameters of interest are $\beta_{1t}, \beta_{2t}, \beta_{3t}$, with $\beta_{1t} \simeq 0$, $\beta_{2t} \simeq 0$, $\beta_{3t} \simeq 0$ providing empirical evidence for the presence of Gibrat's law. A distinctive feature of Equation (23) is the inclusion of age distribution—days since outbreak for each city—in addition to the growth rate. Obtaining age distribution has traditionally been cumbersome in power law analysis. Fortunately, our data conveniently affords us this variable as we observe the entire timeline of the evolution of COVID-19 across Chinese cities.

4.3 | Application

As discussed in Section 4.1, a proportionate random growth model can potentially explain a power law in the data during the early phases of the pandemic. We thus apply the methods reviewed in Section 4.2 to each day between 23 January 2020 and 2 February 2020 (inclusive). The reason for choosing these dates is twofold. First, at least 30 cities had a nonzero number of cumulative cases ($S_{it} > 0$) during that period (see Figure 2). Second, the estimated power law exponent is $\gamma \simeq 1$ between late January and early February (see Figure 7), which is a condition necessary for the validity of a proportionate random growth process, as noted above.

Figure 8 shows the estimation results for ρ_t in Equation (22) for $t = $ Jan 23, $\ldots$, Feb 2. Clearly, the estimates of ρ_t are statistically indistinguishable from unity ($\rho_t \simeq 1$), which confirms the random growth model predicated by Gibrat's law. The 95% confidence interval shrinks moving left
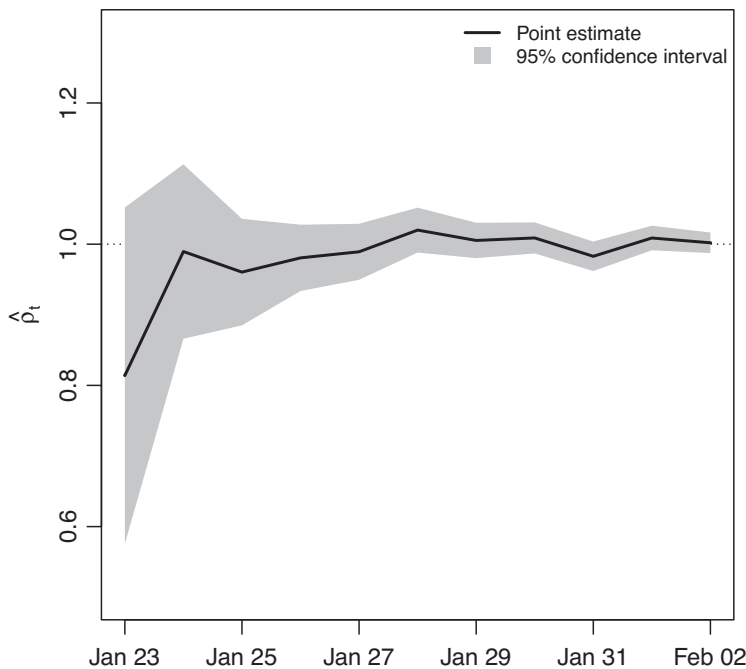

FIGURE 8 Estimates of ρ_t in Equation (22) between 23 January 2020 and 2 February 2020, with 95% confidence bands. $\rho_t \simeq 1$ provides empirical evidence for Gibrat's law
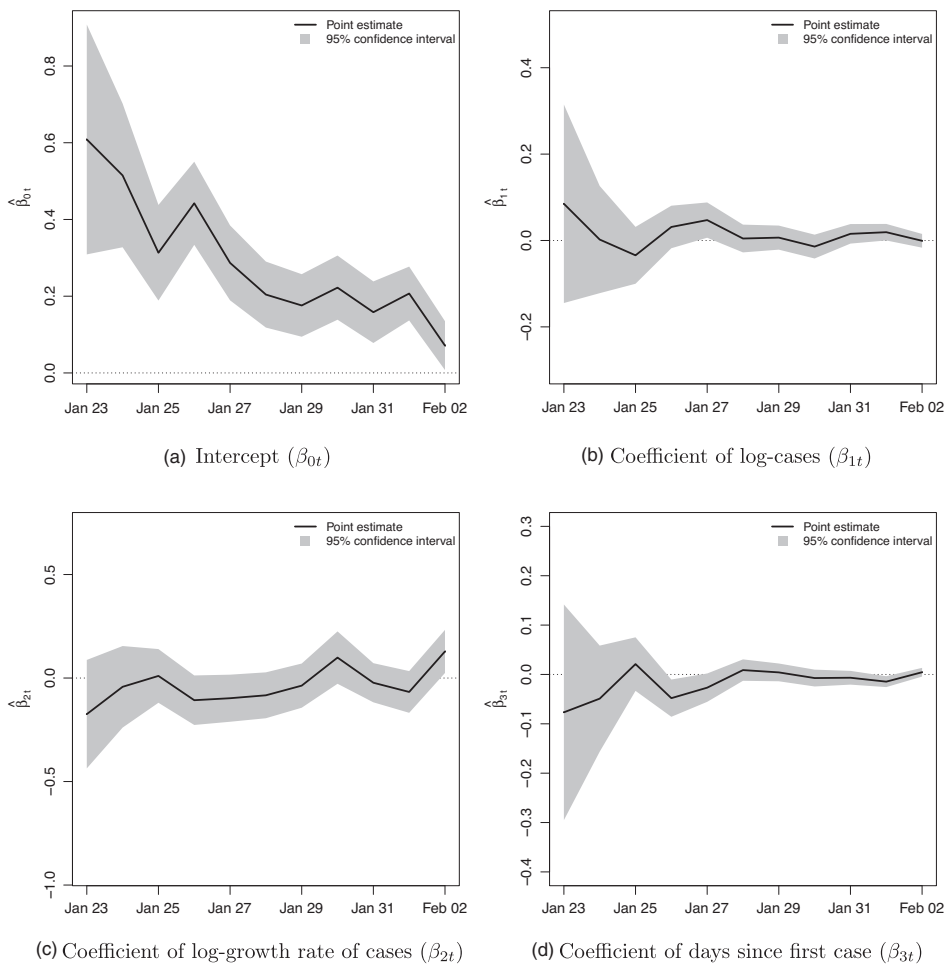
(a) Intercept (β_{0t})

(b) Coefficient of log-cases (β_{1t})

(c) Coefficient of log-growth rate of cases (β_{2t})

(d) Coefficient of days since first case (β_{3t})

FIGURE 9   Estimates of β_{0t}, β_{1t}, β_{2t}, β_{3t} in Equation (23) between 23 January 2020 and 2 February 2020, with 95% confidence bands. The parameters of interest are β_{1t}, β_{2t}, β_{3t}, with $\beta_{1t} \simeq 0$, $\beta_{2t} \simeq 0$, $\beta_{3t} \simeq 0$ providing empirical evidence for Gibrat's law

to right, which can be attributed to increasing sample size (i.e. increasing number of cities with confirmed cases) over time (see Figure 2).

Figure 9 reports the estimation results for β_{0t}, β_{1t}, β_{2t}, β_{3t} in Equation (23) for $t =$ Jan 23, ... , Feb 2. Panels (b)–(d) contain the estimates for β_{1t}, β_{2t}, β_{3t}, which are of primary interest here. It is apparent that these estimates are mostly equal to zero ($\beta_{1t} \simeq 0$, $\beta_{2t} \simeq 0$, $\beta_{3t} \simeq 0$), which indicates the growth rate between days t and $t + 1$ does not depend on the number of cases on day t, nor on the growth rate between days $t - 1$ and t, nor on the number of days since the first confirmed case. This provides strong evidence for the existence of Gibrat's law for COVID-19 cases in Chinese cities during the period under consideration. The estimates of β_{0t} in panel (a) show that the expected growth rate of confirmed cases was indeed positive between 23 January and 2 February, with a general downward trend.

In summary, confirmation of Gibrat's law provides support for a proportionate random growth model as a plausible power law generating mechanism for COVID-19 cases in China in the early phases of the outbreak, when the number of cases was still rising. In addition, confirmation of Gibrat's law implies that COVID-19 cases in Chinese cities grew proportionately during the early

phases of the pandemic (when the number of cases was rising), with the underlying stochastic process remaining the same for all cities. This means each city's COVID-19 growth rate was drawn randomly and independently of its size. In the later phases of the outbreak, as the number of cumulative cases starts to stabilize, a proportionate random growth model becomes less plausible, as $\mathbb{E}(\mu_{it}) = 1$ in Equation (15), hence the underlying stochastic process is no longer the same for all cities.

5 | CONCLUSION

The dynamics of the novel coronavirus pandemic are complex and determined by a myriad of factors, which are yet to be fully understood. In spite of the apparent chaotic evolution of the pandemic, surprising regularities can still be observed in the size distribution and growth process of COVID-19 cases. In this article, we examined the distribution of the novel coronavirus cases in China—the original epicentre of the ongoing pandemic. We presented empirical evidence for a power law distribution for the upper tail of the number of COVID-19 cases in Chinese cities. The power law fit is robust to different estimation methods, passes rigorous diagnostic tests, and fits the data better than a number of natural alternatives. As such, the power law surmounts the statistical hurdle.

The implications of the power law fit are that (i) the number of COVID-19 cases in Chinese cities is heavy tailed and disperse; (ii) mean and variance are generally not finite, so that average number of COVID-19 cases is problematic to talk about; and (iii) COVID-19 cases are concentrated within a few cities that account for a disproportionately large amount of infections. Admittedly, there may always be a distribution that fits the data better than a power law granted that there are virtually an infinite number of distributions. What we showed in this study is that the power law distribution is able to capture the upper tail of the data, and better than several 'go-to' distributions. This has important implications for empirical work as, for reliable analysis of the effects of COVID-19 pandemic, using econometrically justified and robust methods that account for potential heavy tailedness and tail risk property is in order.

DATA AVAILABILITY STATEMENT
The data used in the study is publicly available. The data sources are mentioned in the article.

ORCID
Sherzod B. Akhundjanov https://orcid.org/0000-0003-3372-3574

REFERENCES
Ahundjanov, B.B. & Akhundjanov, S.B. (2019) Gibrat's law for CO2 emissions. *Physica A: Statistical Mechanics and its Applications*, 526, 120944.

Akhundjanov, S.B. & Chamberlain, L. (2019) The power law distribution of agricultural land size. *Journal of Applied Statistics*, 46(16), 3044–3056.

Akhundjanov, S.B. & Drugova, T. (2021) On the growth process of U.S. agricultural land. *Empirical Economics*, in press.

Akhundjanov, S.B. & Toda, A.A. (2020) Is Gibrat's 'Economic Inequality' lognormal? *Empirical Economics*, 59(5), 2071–2091.

Akhundjanov, S.B., Devadoss, S. & Luckstead, J. (2017) Size distribution of national CO2 emissions. *Energy Economics*, 66, 182–193.

Axtell, R.L. (2001) Zipf distribution of US firm sizes. *Science*, 293(5536), 1818–1820.

Bak, P. & Tang, C. (1989) Earthquakes as a self-organized critical phenomenon. *Journal of Geophysical Research*, 94(B11), 15635–15637.

Balthrop, A. (2016) Power laws in oil and natural gas production. *Empirical Economics*, 51(4), 1521–1539.

Battistin, E., Blundell, R. & Lewbel, A. (2009) Why is consumption more log normal than income? Gibrat's law revisited. *Journal of Political Economy*, 117(6), 1140–1154.

Beare, B.K. & Toda, A.A. (2020) On the emergence of a power law in the distribution of COVID-19 cases. *arXiv preprint arXiv:2004.12772*.

Benhabib, J., Bisin, A. & Zhu, S. (2011) The distribution of wealth and fiscal policy in economies with finitely lived agents. *Econometrica*, 79(1), 123–157.

Berliant, M. & Watanabe, H. (2015) Explaining the size distribution of cities: extreme economies. *Quantitative Economics*, 6(1), 153–187.

Blasius, B. (2020) Power law distribution in the number of confirmed COVID-19 cases. *arXiv preprint arXiv:2004.00940*.

Champernowne, D.G. (1953) A model of income distribution. *The Economic Journal*, 63(250), 318–351.

China Data Lab. (2020) China COVID-19 daily cases with basemap. Harvard Dataverse, Available from: https://doi.org/10.7910/DVN/MR5IJN

Clauset, A., Shalizi, C.R. & Newman, M.E.J. (2009) Power law distributions in empirical data. *SIAM Review*, 51(4), 661–703.

Cucinotta, D. & Vanelli, M. (2020) WHO declares COVID-19 a pandemic. *Acta Bio-Medica: Atenei Parmensis*, 91(1), 157–160.

Devadoss, S., Luckstead, J., Danforth, D. & Akhundjanov, S. (2016) The power law distribution for lower tail cities in India. *Physica A: Statistical Mechanics and its Applications*, 442, 193–196.

Distaso, W., Ibragimov, R., Semenov, A. & Skrobotov, A. (2020) COVID-19: tail risk and predictive regressions. *arXiv preprint arXiv:2009.02486*.

Eeckhout, J. (2004) Gibrat's law for (all) cities. *American Economic Review*, 94(5), 1429–1451.

Farmer, D.J., Gillemot, L., Lillo, F., Mike, S. & Sen, A. (2004) What really causes large price changes? *Quantitative Finance*, 4(4), 383–397.

Gabaix, X. (1999) Zipf's law for cities: an explanation. *The Quarterly Journal of Economics*, 114(3), 739–767.

Gabaix, X. (2009) Power laws in economics and finance. *Annual Review of Economics*, 1(1), 255–294.

Gabaix, X. (2016) Power laws in economics: an introduction. *Journal of Economic Perspectives*, 30(1), 185–206.

Gabaix, X. & Ibragimov, R. (2011) Rank - 1/2: a simple way to improve the OLS estimation of tail exponents. *Journal of Business & Economic Statistics*, 29(1), 24–39.

Gibrat, R. (1931) *Les inegalites economiques*. Paris: Librairie du Recueil Sirey.

Giesen, K., Zimmermann, A. & Suedekum, J. (2010) The size distribution across all cities—double Pareto lognormal strikes. *Journal of Urban Economics*, 68(2), 129–137.

González-Val, R. & Sanso-Navarro, M. (2010) Gibrat's law for countries. *Journal of Population Economics*, 23(4), 1371–1389.

Han, Y., Liu, Y., Zhou, L., Chen, E., Liu, P., Pan, X. et al. (2020) Epidemiological assessment of imported coronavirus disease 2019 (COVID-19) cases in the most affected city outside of Hubei Province, Wenzhou, China. *JAMA Network Open*, 3(4), e206785.

Hill, B.M. (1975) A simple general approach to inference about the tail of a distribution. *The Annals of Statistics*, 3(5), 1163–1174.

Ioannides, Y.M. & Overman, H.G. (2003) Zipf's law for cities: an empirical examination. *Regional Science and Urban Economics*, 33(2), 127–137.

Ioannides, Y. & Skouras, S. (2013) US city size distribution: robustly Pareto, but only in the tail. *Journal of Urban Economics*, 73(1), 18–29.

Irmay, S. (1997) The relationship between Zipf's law and the distribution of first digits. *Journal of Applied Statistics*, 24(4), 383–394.

Keitt, T.H. & Stanley, H.E. (1998) Dynamics of North American breeding bird populations. *Nature*, 393(6682), 257–260.

Klass, O.S., Biham, O., Levy, M., Malcai, O. & Solomon, S. (2006) The Forbes 400 and the Pareto wealth distribution. *Economics Letters*, 90(2), 290–295.

Krugman, P. (1996) *The self-organizing economy*. Cambridge, MA: Blackwell.

Luckstead, J. & Devadoss, S. (2017) Pareto tails and lognormal body of US cities size distribution. *Physica A: Statistical Mechanics and its Applications*, 465, 573–578.

Luttmer, E.G.J. (2007) Selection, growth, and the size distribution of firms. *The Quarterly Journal of Economics*, 122(3), 1103–1144.

Malamud, B.D., Morein, G. & Turcotte, D.L. (1998) Forest fires: an example of self-organized critical behavior. *Science*, 281(5384), 1840–1842.

Mitzenmacher, M. (2004) A brief history of generative models for power law and lognormal distributions. *Internet Mathematics*, 1(2), 226–251.

Newman, M.E.J. (2005) Power laws, Pareto distributions and Zipf's law. *Contemporary Physics*, 46(5), 323–351.

Nigai, S. (2017) A tale of two tails: productivity distribution and the gains from trade. *Journal of International Economics*, 104, 44–62.

Pareto, V. (1896) *Cours d'économie politique professé al'Université de Lausanne*, vol. I. Paris: F. Rouge.

Patel, R.D. & Schoenberg, F.P. (2011) A graphical test for local self-similarity in univariate data. *Journal of Applied Statistics*, 38(11), 2547–2562.

Perline, R. (2005) Strong, weak and false inverse power laws. *Statistical Science*, 20(1), 68–88.

Plerou, V., Amaral, L.A.N., Gopikrishnan, P., Meyer, M. & Stanley, H.E. (1999) Similarities between the growth dynamics of university research and of competitive economic activities. *Nature*, 400(6743), 433–437.

Reed, W.J. (2001) The Pareto, Zipf and other power laws. *Economics Letters*, 74(1), 15–19.

Rose, A.K. (2006) Cities and countries. *Journal of Money, Credit, and Banking*, 38(8), 2225–2246.

Singh, S.K. & Maddala, G.S. (1976) A function for size distribution of incomes. *Econometrica*, 44(5), 963–970.

Sornette, D. (2006) *Critical phenomena in natural sciences*. New York: Springer.

Stanley, M.H.R., Buldyrev, S.V., Havlin, S., Mantegna, R.N., Salinger, M.A. & Stanley, H.E. (1995) Zipf plots and the size distribution of firms. *Economics Letters*, 49(4), 453–457.

Sutton, J. (1997) Gibrat's legacy. *Journal of Economic Literature*, 35(1), 40–59.

Toda, A.A. (2012) The double power law in income distribution: explanations and evidence. *Journal of Economic Behavior & Organization*, 84(1), 364–381.

Toda, A.A. (2017) A note on the size distribution of consumption: more double Pareto than lognormal. *Macroeconomic Dynamics*, 21(6), 1508–1518.

Toda, A.A. & Walsh, K. (2015) The double power law in consumption and implications for testing Euler equations. *Journal of Political Economy*, 123(5), 1177–1200.

United Nations (2018) World Urbanization Prospects: The 2018 Revision. Population Division, Department of Economic and Social Affairs, United Nations.

Voitalov, I., van der Hoorn, P., van der Hofstad, R. & Krioukov, D. (2019) Scale-free networks well done. *Physical Review Research*, 1(3), 033034.

Wold, H.O.A. & Whittle, P. (1957) A model explaining the Pareto distribution of wealth. *Econometrica*, 25(4), 591–595.

Zhu, N., Zhang, D., Wang, W., Li, X., Yang, B., Song, J. et al. (2020) A novel coronavirus from patients with pneumonia in China, 2019. *The New England Journal of Medicine*, 382, 727–733.

Zipf, G.K. (1949) *Human behavior and the principle of least effort*. Cambridge, MA: Addison-Wesley.